

## Supporting Information

# Effects of temperature and coating speed on the morphology of solution-sheared halide perovskite thin-film

*Min Kyu Kim<sup>1‡</sup>, Hyeon Seok Lee<sup>1‡</sup>, Seong Ryul Pae<sup>1</sup>, Dong-Jun Kim<sup>2</sup>, Jung-Yong Lee<sup>2</sup>, Issam Gereige<sup>3</sup>, Steve Park<sup>1\*</sup>, and Byungha Shin<sup>1\*</sup>*

<sup>1</sup>Department of Materials Science and Engineering, Korea Advanced Institute of Science and Technology, Daejeon, 34141, Korea

<sup>2</sup>Graduate School of Energy, Environment, Water, and Sustainability (EEWS), Korea Advanced Institute of Science and Technology, Daejeon, 34141, Korea

<sup>3</sup>Saudi Aramco Research & Development Center, Dhahran 31311, Kingdom of Saudi Arabia

### AUTHOR INFORMATION

#### **Corresponding Author**

E-mail: : [stevepark@kaist.ac.kr](mailto:stevepark@kaist.ac.kr) , [byungha@kaist.ac.kr](mailto:byungha@kaist.ac.kr)

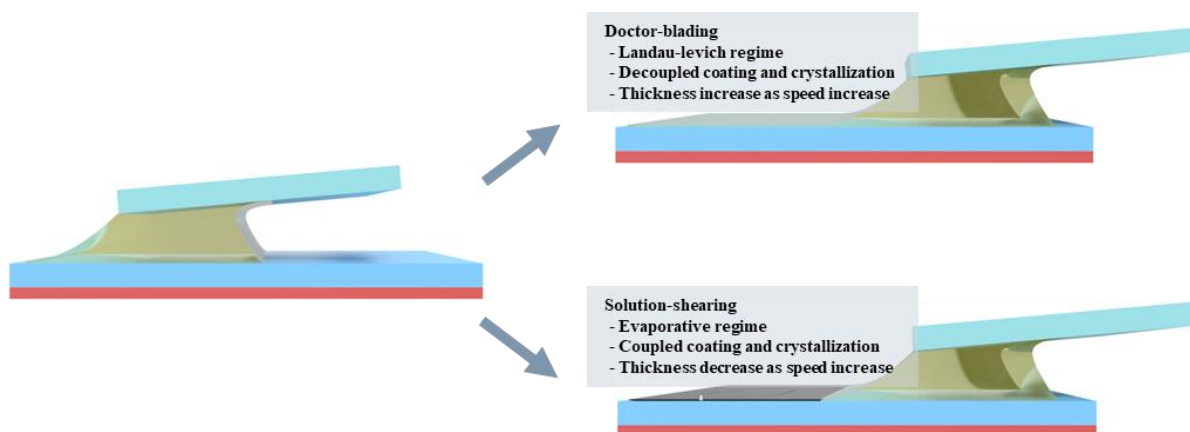
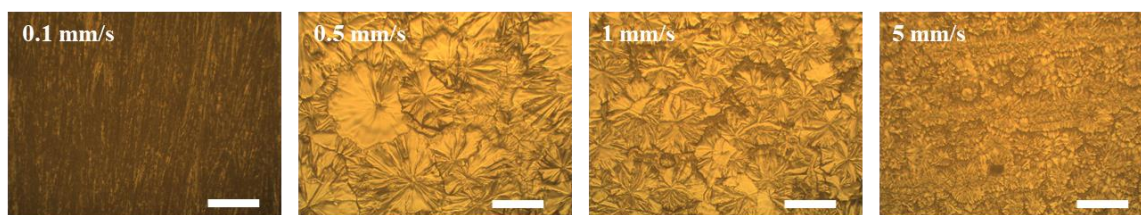


**Figure S1.** Difference between solution-shearing and doctor-blading. Solution-shearing and doctor-blading share similarities in that they both use a blade to deposit thin-film onto a substrate. However, solution-shearing is typically conducted under “evaporation regime”, where solution coating and crystallization occur simultaneously. On the other hand, doctor-blading takes place in Landau-levich regime where crystallization is decoupled from solution coating; in other words, crystallization occurs after the formation of solution liquid layer. In this case, the thickness of the thin-film increases with increasing coating speed because fluid viscosity dominates over its surface tension (high capillary number). On the contrary, in solution-shearing, surface tension dominates the fluid characteristics. In this case, film thickness decreases with increasing coating speed, which is what was observed in our experiments. In the evaporative regime, solvent evaporation rate and the supply of solution to the drying front (i.e. near the contact line) via capillary flow and Marangoni flow determines the rate and degree of supersaturation, through which crystallization can be controlled.

**FTO/NiO<sub>x</sub>/MAPbI<sub>3</sub>**



**FTO/PEDOT:PSS/MAPbI<sub>3</sub>**

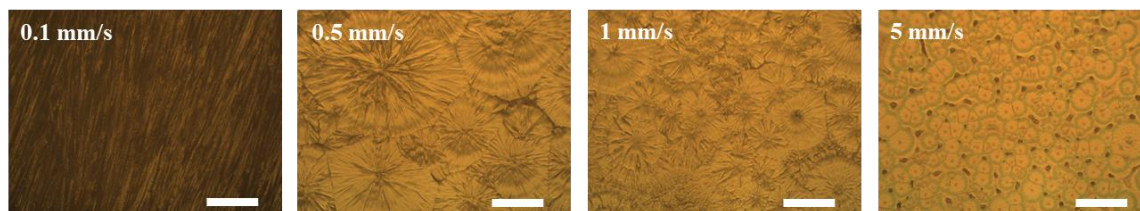


**Figure S2.** Optical microscopy images of solution-sheared MAPbI<sub>3</sub> film on different substrates. Substrate temperature was fixed to 110 °C where phase transition is prominently observed.

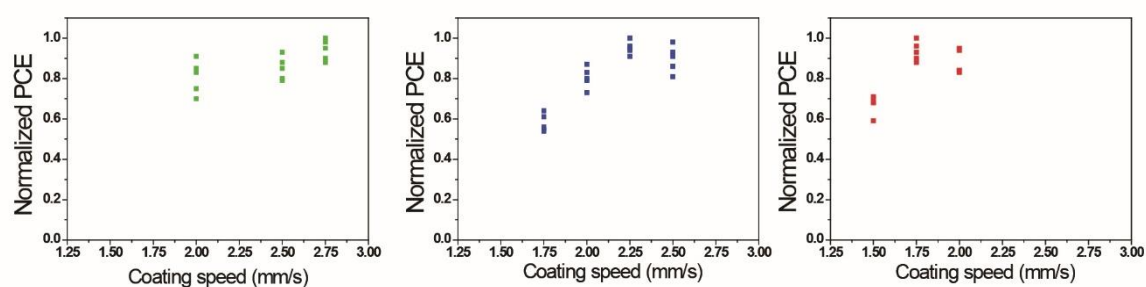


**Figure S3.** Normalized PCE versus coating speed for different ratios of DMF:DMSO. (a) 7:3, (b) 5:5, (c) 4:6. Concentration was fixed to 1M for all of the samples. DMSO was previously used as a solvent for blade coating perovskite thin film, which yielded high performance solar cells.<sup>2</sup> DMSO has a relatively low vapor pressure (0.049 kPa at 20 °C) and boiling point (189 °C); hence, it evaporates relatively slowly during solution-shearing. To obtain phase 3 thin film using DMSO, the coating speed needs to be relatively slow ( $\sim 12 \mu\text{m/s}$ ).<sup>2</sup> If the coating speed is too high, the meniscus protrudes far from the blade, resulting in thin films obtained phase 4. Since DMF has a comparatively high vapor pressure (0.38 kPa at 20 °C) and boiling point (153 °C), it has a higher solvent evaporation rate compared to DMSO. Hence, higher ratio of DMF:DMSO shifts the optimum PCE to higher coating speeds, as seen in the plots above. Using pure DMF, however, is not ideal since this requires coating speeds that are too high ( $\sim 10 \text{ mm/s}$ ). Generally, at high coating speeds, pinholes are generated in the film.<sup>3</sup> On the other hand, under slow coating speeds, DMF can evaporate faster than the rate at which the blade moves, resulting in the gradual depletion of meniscus. Eventually, perovskite crystals begin to form on or near the blade, which are then dragged across the substrate. We therefore used a mixture of DMF:DMSO as our solvent, and used a volume ratio of 7:3 for our experiments to maximize the coating speed without compromising the quality of the films.

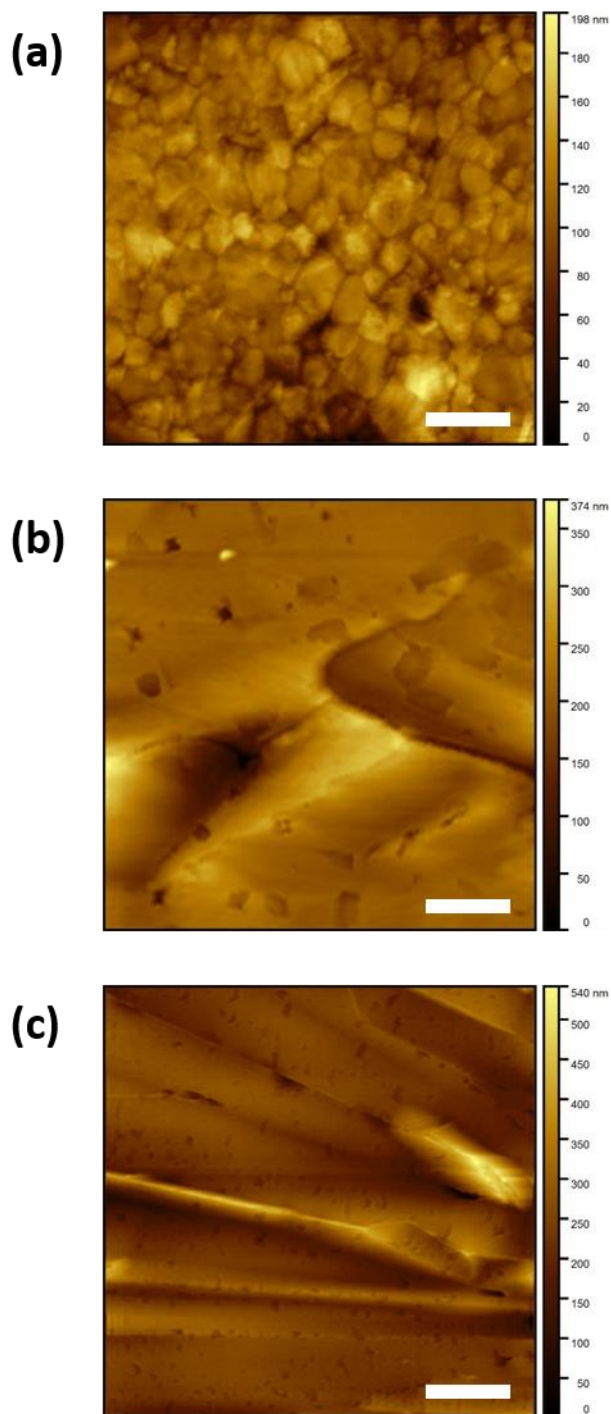


**Figure S4.** AFM images of (a) spin-coated and (b,c) solution-sheared (2.75 mm/s, 150 °C) MAPbI<sub>3</sub> films. Root-mean-square (rms) roughness of the images were 20 nm, 24 nm, and 64 nm, respectively. Scale bars are 2 μm, 2 μm, and 10 μm for (a), (b), (c), respectively.

### **Additional Analysis of Figure 2c (XRD)**

According to a previous report,<sup>1</sup> under slow evaporation rate, a relatively high amount of  $\text{PbI}_2$  was observed in the film. This can be attributed to the fact that under slow evaporation rate (as in phase 2) and temperature below 100 °C, there is greater loss of MAI due to vaporization before it reacts with  $\text{PbI}_2$ . The comparatively higher solvent evaporation rate (hence higher supersaturation rate) in the other phases, due to high temperature above 100 °C, result in almost all of the MAI to react with  $\text{PbI}_2$ ; hence, little or no  $\text{PbI}_2$  peak is observed. Fast coating mode (5.00 mm/s) of phase 2 also did not show any peak from  $\text{PbI}_2$  since high surface to volume ratio (i.e. fast coating speed) facilitates rapid solvent evaporation.

In phase 1, the intermediate phase peaks (diamond) are relatively intense compared to other phases. The position of the peaks suggest that these peaks correspond to  $\text{PbI}_2$ -MAI-DMF-DMSO solvate state.<sup>1</sup> As explained in the main text, for phase 1, slow solvent evaporation rate combined with sufficient supply of solution to the meniscus line yields the formation of solvate more likely compared to the other phases.

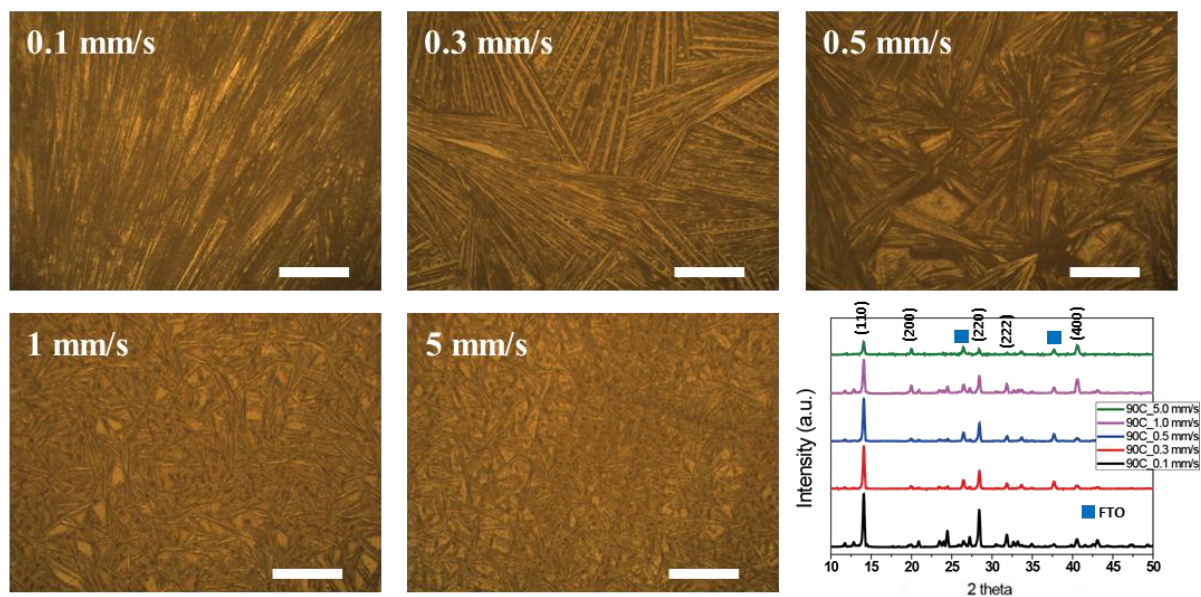


**Figure S5.** Optical microscopy images of solution-sheared MAPbI<sub>3</sub> film coated at different coating speeds and their XRD data at substrate temperature of 90 °C. Observed morphologies are well consistent with phase mapping in Figure 1b. Phase 1 is observed in the 0.1 mm/s sample. Above 0.3 mm/s, microwire size decreases as coating speed increases, showing phase 2 morphology. (110) and (220) XRD peak intensities decrease as film thickness gets thinner with increasing coating speed.

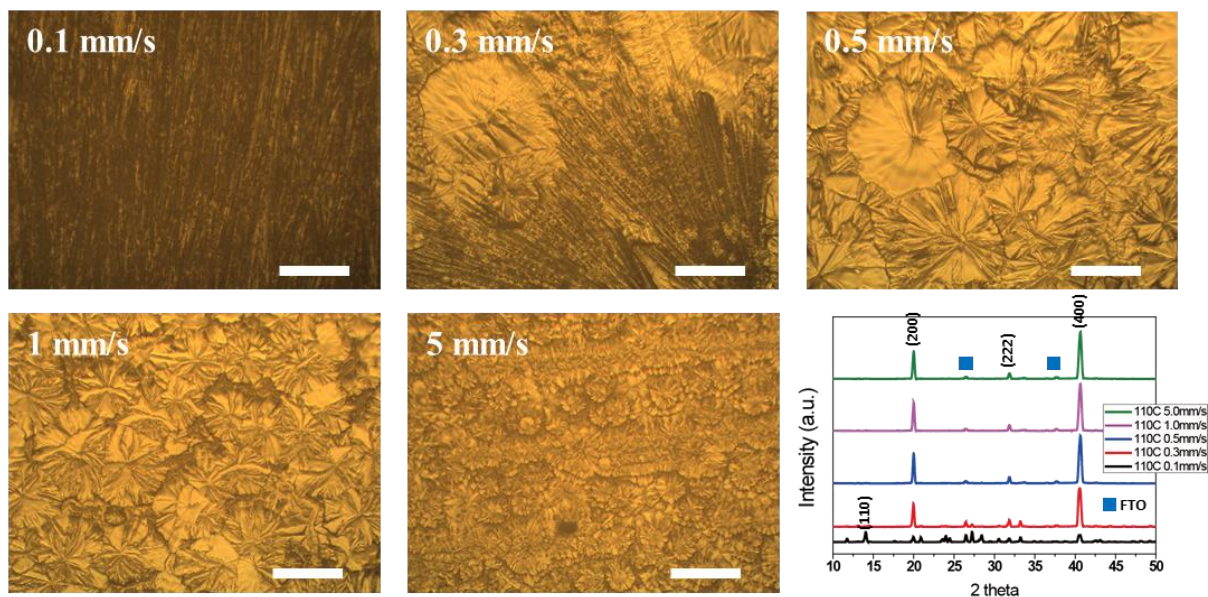


**Figure S6.** Optical microscopy images of solution-sheared MAPbI<sub>3</sub> film coated at different coating speeds and their XRD data at substrate temperature of 110 °C. Observed morphologies are consistent with phase mapping in Figure 1b. Phase 1 is observed in 0.1 mm/s sample. Phase 2 (microwires) and phase 3 (close packed domain) co-existing in 0.3 mm/s, where phase transformation occurs. Phase 3 is observed for 0.5 mm/s and 1 mm/s sample. Phase 4 is observed in the 5 mm/s sample. Phase transformation from 2 to 3 can be confirmed with XRD data; above 0.3 mm/s, (110) and (220) peak intensities decrease, while (200) and (400) peak intensities increase.

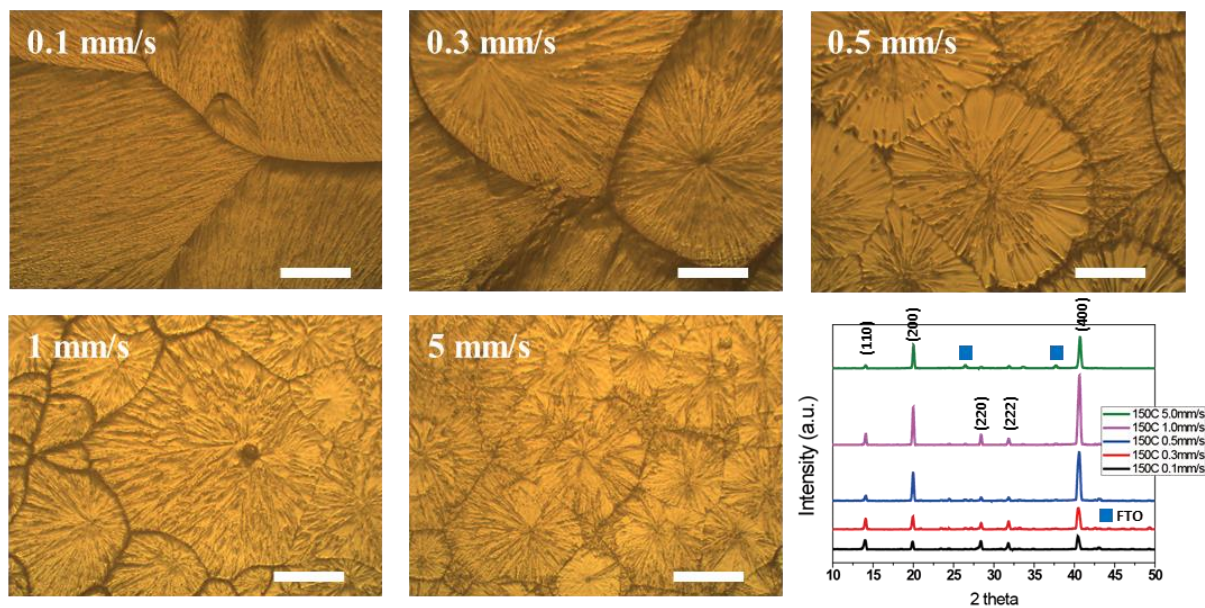


**Figure S7.** Optical microscopy images of solution-sheared MAPbI<sub>3</sub> film coated at different coating speeds and their XRD data at substrate temperature of 150 °C. Phase 3 was observed at all coating speeds (from 0.1 mm/s to 5 mm/s). The domain size decreases as coating speed increases. (200) and (400) peak intensities from XRD increases with coating speed until 1.0 mm/s although film thickness is found to decrease with coating speed. XRD data between 1.0 mm/s and 5.0 mm/s is shown on Figure 4a.

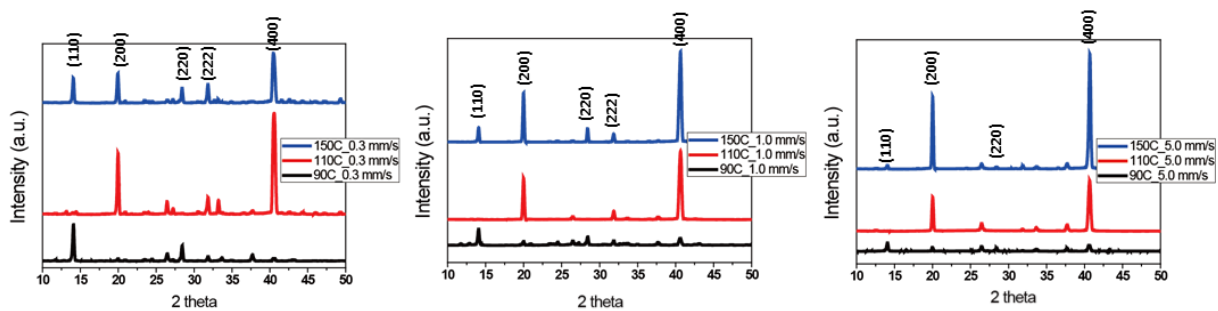


**Figure S8.** Comparison of XRD analysis from solution-sheared MAPbI<sub>3</sub> film at the same coating speed under different substrate temperatures.

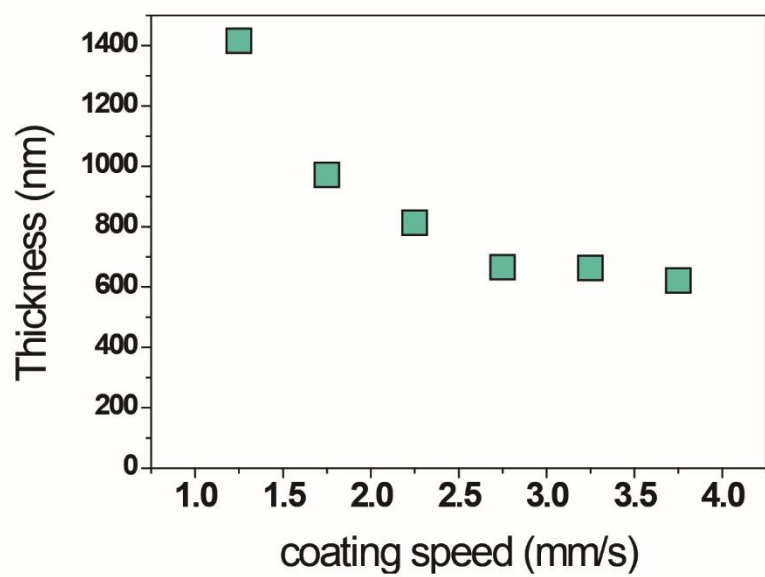


**Figure S9.** Thickness of solution-sheared MAPbI<sub>3</sub> film coated at different coating speeds.

Substrate temperature was fixed at 150 °C.

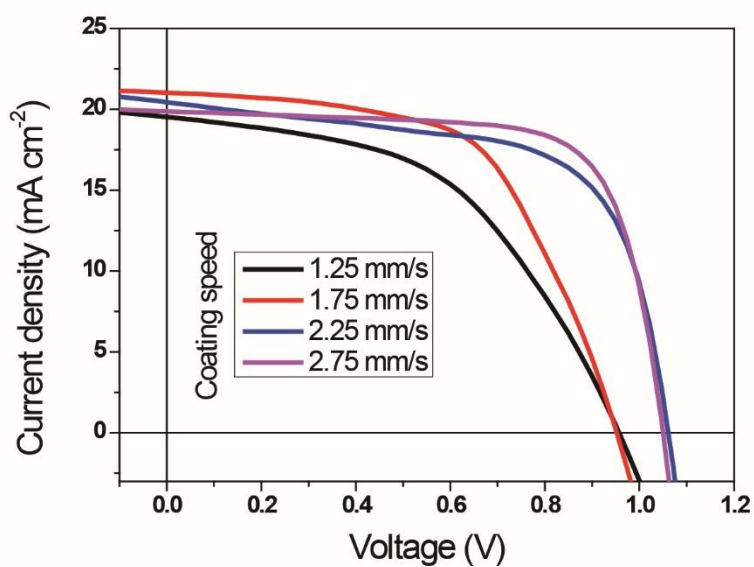


**Figure S10.** J-V curve of perovskite solar cells made with perovskite films at different coating speeds. Device structure: FTO/NiO<sub>x</sub>/MAPbI<sub>3</sub>/PCBM/BCP/Ag. Substrate temperature was fixed at 150 °C.

Cell number	V <sub>oc</sub> (V)	J <sub>sc</sub> (mA/cm <sup>2</sup> )	FF (%)	PCE (%)
1	1.049	19.87	72.18	15.06
2	1.054	20.81	68.18	14.96
3	1.051	20.06	70.50	14.88
4	1.054	20.28	66.75	14.28
5	1.055	20.75	64.76	14.19
6	1.059	20.09	63.42	13.50
7	1.055	20.34	61.94	13.30
8	1.051	20.27	69.43	14.79
9	1.044	20.31	66.15	14.03
10	1.041	19.98	66.05	13.74

**Table S1.** Photovoltaic parameters of two solution-sheared samples (2.5 cm x 2.5 cm), each having 5 devices. Coating speed was 2.75 mm/s and the substrate temperature was 150 °C. Device structure is as follows: FTO/NiO<sub>x</sub>/MAPbI<sub>3</sub>/PCBM/BCP/Ag. Aperture area for each cell was 0.1 cm<sup>2</sup>.

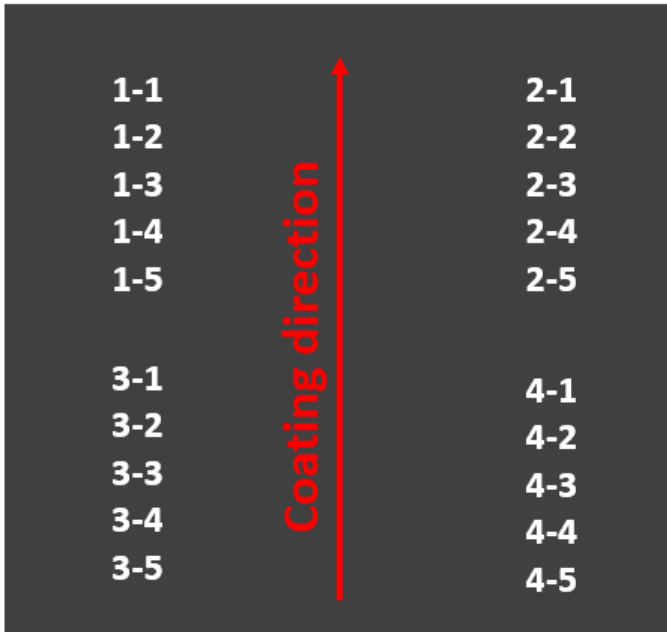


**Table S2.** Photovoltaic parameters of a large area (57 cm<sup>2</sup>) solution-sheared perovskite film at various regions. The film was cut into four sections each having 2.5 x 2.5 cm<sup>2</sup> area, and each section contained 5 devices. The coating speed was 2.75 mm/s and the substrate temperature was 150 °C. Device structure is as follows: FTO/NiO<sub>x</sub>/MAPbI<sub>3</sub>/C60/BCP/Ag. Aperture area for each cell is 0.1 cm<sup>2</sup>.

<b>Shearing Device</b>	<b>V<sub>o8c</sub></b> <b>(V)</b>	<b>J<sub>sc</sub></b> <b>(mA/cm<sup>2</sup>)</b>	<b>FF</b> <b>(%)</b>	<b>PCE</b> <b>(%)</b>
1-1	0.931	21.18	52.46	10.35
1-2	0.944	21.21	52.15	10.44
1-3	0.945	20.97	52.72	10.45
1-4	0.919	21.67	50.42	10.04
1-5	0.968	21.62	54.00	11.31
2-1	0.916	21.41	55.12	10.82
2-2	0.945	21.50	52.08	10.59
2-3	0.937	21.43	54.25	10.90
2-4	0.930	21.31	58.07	11.51
2-5	0.922	21.48	56.35	11.17
3-1	0.921	21.09	56.71	11.02
3-2	0.913	21.11	57.96	11.18
3-3	0.905	21.15	59.27	11.35
3-4	0.906	20.95	53.83	10.23
3-5	0.906	21.03	57.05	10.88
4-1	0.890	21.12	58.86	11.12
4-2	0.918	20.81	53.07	10.15
4-3	0.909	20.78	58.11	10.99
4-4	0.882	21.24	59.44	11.14
4-5	0.900	21.03	61.00	11.55

## References

- (1) Zhong, Y.; Munir, R.; Li, J.; Tang, M.-C.; Niazi, M. R.; Smilgies, D.-M.; Zhao, K.; Amassian, A., Blade-Coated Hybrid Perovskite Solar Cells with Efficiency > 17%: An In Situ Investigation. *ACS Energy Letters* **2018**, 3 (5), 1078-1085.
- (2) He, M.; Li, B.; Cui, X.; Jiang, B.; He, Y.; Chen, Y.; O'Neil, D.; Szymanski, P.; Ei-Sayed, M. A.; Huang, J.; Lin, Z., Meniscus-assisted solution printing of large-grained perovskite films for high-efficiency solar cells. *Nature communications* **2017**, 8, 16045.
- (3) Deng, Y.; Zheng, X.; Bai, Y.; Wang, Q.; Zhao, J.; Huang, J., Surfactant-controlled ink drying enables high-speed deposition of perovskite films for efficient photovoltaic modules. *Nature Energy* **2018**.